Density-Functional Study of Mechanisms for the Cofactor-Free Decarboxylation Performed by Uroporphyrinogen III Decarboxylase

Pedro J. Silva[†] and Maria João Ramos*[,‡]

Faculdade de Ciências da Saúde, Universidade Fernando Pessoa, Rua Carlos da Maia, 296, 4200-150 Porto, Portugal, and Faculdade de Ciências do Porto, REQUIMTE, Rua do Campo Alegre, 687, 4169-007 Porto, Portugal

Received: April 7, 2005; In Final Form: July 11, 2005

Uroporphyrinogen III decarboxylase catalyzes the fifth step in heme biosynthesis: the elimination of carboxyl groups from the four acetate side chains of uroporphyrinogen III to yield coproporphyrinogen III. The enzyme acts by successively protonating each of the four pyrrole rings present in the substrate, thereby allowing decarboxylation of their side chains, but the identity of the proton donors has not been established yet. Tyr164 has been suggested as a proton donor, and Asp86 has been proposed to act either as a proton donor or as an intermediate-stabilizing residue. We have performed density-functional calculations to study this reaction mechanism, and found that the rate-limiting step is substrate protonation, rather than decarboxylation. Surprisingly, whereas Tyr164 is unable to protonate the substrate, this protonation can be effected by a nearby arginine residue (Arg37), with a free energy barrier of 21.4 kcal·mol^{-1}, in remarkable agreement with the experimental value of 19.5 kcal·mol^{-1}. The central positioning of this residue in close proximity to all four pyrrole rings in the substrate may play a key role in the sequential activation of each of these moieties.

I. Introduction

The porphyrias are metabolic disorders in which the activities of the enzymes in the heme biosynthetic pathway are partially or almost totally deficient, leading to tissue accumulation and excessive excretion of porphyrins or their precursors. These products are not only useless, but also toxic, and the ensuing diseases can be neurological or photosensitive, depending on the principal site of expression of the specific enzymatic defect.[1] The most common porphyria in humans is porphyria cutanea tarda (PCT), which results from the accumulation of uroporphyrin and partially decarboxylated intermediates in the liver, plasma, and skin and is characterized by severe photosensitive dermatosis, hypertrichosis, and hyperpigmentation.[2] Present treatment relies on frequent phlebotomy and on chloroquine administration, which stimulates excretion of excess porphyrins.[1]

The origin of the disease has been traced to the impairment of the key enzyme uroporphyrinogen III decarboxylase (UroD), which catalyzes the fifth step in heme biosynthesis: the elimination of carboxyl groups from the four acetate side chains of uroporphyrinogen III to yield coproporphyrinogen III[1] (Figure 1). At low substrate concentrations the reaction is believed to follow an ordered route, with the sequential removal of CO_2 from the D, A, B, and C rings,[3] whereas at higher substrate/enzyme levels a random route seems to be operative.[4] The enzyme functions as a dimer in solution, and both the enzymes from human[5] and tobacco[6] have been crystallized and solved at good resolutions. UroD is quite an unusual decarboxylase, since it performs decarboxylations without the intervention of any cofactors, unlike the vast majority of decarboxylases. Akthtar[7] has proposed that protonation of the pyrrole ring by an acidic residue will enable it to act as an electron sink, thereby enabling the decarboxylation. A second protonation of the pyrrole ring, followed by the return of the first proton to the original acidic residue, would yield the desired product (Figure 2A).

However, the proton donors have not been identified: modeling of the substrate into the structure of tobacco UroD (Martins' model[6]) suggested that the protons might come from Tyr164 and Asp86, while in the solution structure of substrate-bound human UroD (Phillips' model[5]) Asp86 stabilizes the positive charge in intermediate 1 (see Figure 2C), and no obvious proton donors are apparent. However, a very flexible basic side chain (Arg37) lies close to the substrate and we wondered whether this residue might fulfill the role of a general acid, since the enzyme is inactivated by the arginine-modifying reagent phenylglyoxal.[4] To test these hypotheses, we carried out density-functional calculations of the reaction mechanism on both systems. Our data allow a full overview of the complete reaction mechanism of this intriguing enzyme.

II. Methods

All calculations were performed at the Becke3LYP level of theory.[8−10] In geometry optimizations a medium-sized basis set, 6-31G(d), was used, since it is well-known that larger basis sets give very small additional corrections to the geometries, and their use for this end is hence considered unnecessary from a computational point of view.[11−14] More accurate energies of the optimized geometries were calculated with a triple-ζ quality basis set, 6-311+G(d,p). Our calculations focused on the decarboxylation of pyrrole ring D of uroporphyrinogen III, since this is believed to be the first ring to undergo decarboxylation under physiological conditions.[3] To prevent unrealistic movements of the modeled amino acid side chains, amino acid Cα and Cβ carbon atoms were constrained to their crystallographic positions. Likewise, the intervening substrate pyrrole ring D was also anchored to its initial coordinates by freezing two of its

* Corresponding author. E-mail: mjramos@fc.up.pt.
[†] Universidade Fernando Pessoa.
[‡] REQUIMTE.

10.1021/jp051792s CCC: $30.25
Published on Web 09/01/2005

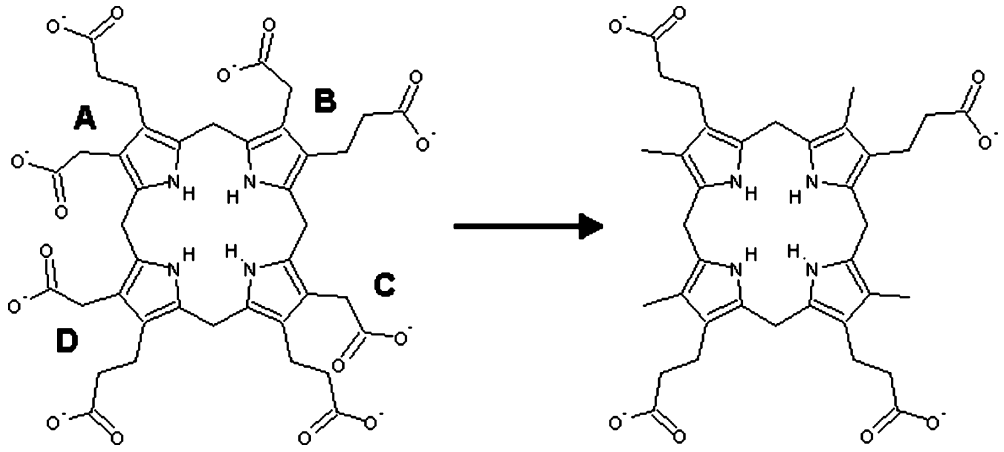

Figure 1. Reaction catalyzed by uroporphyrinogen III decarboxylase.

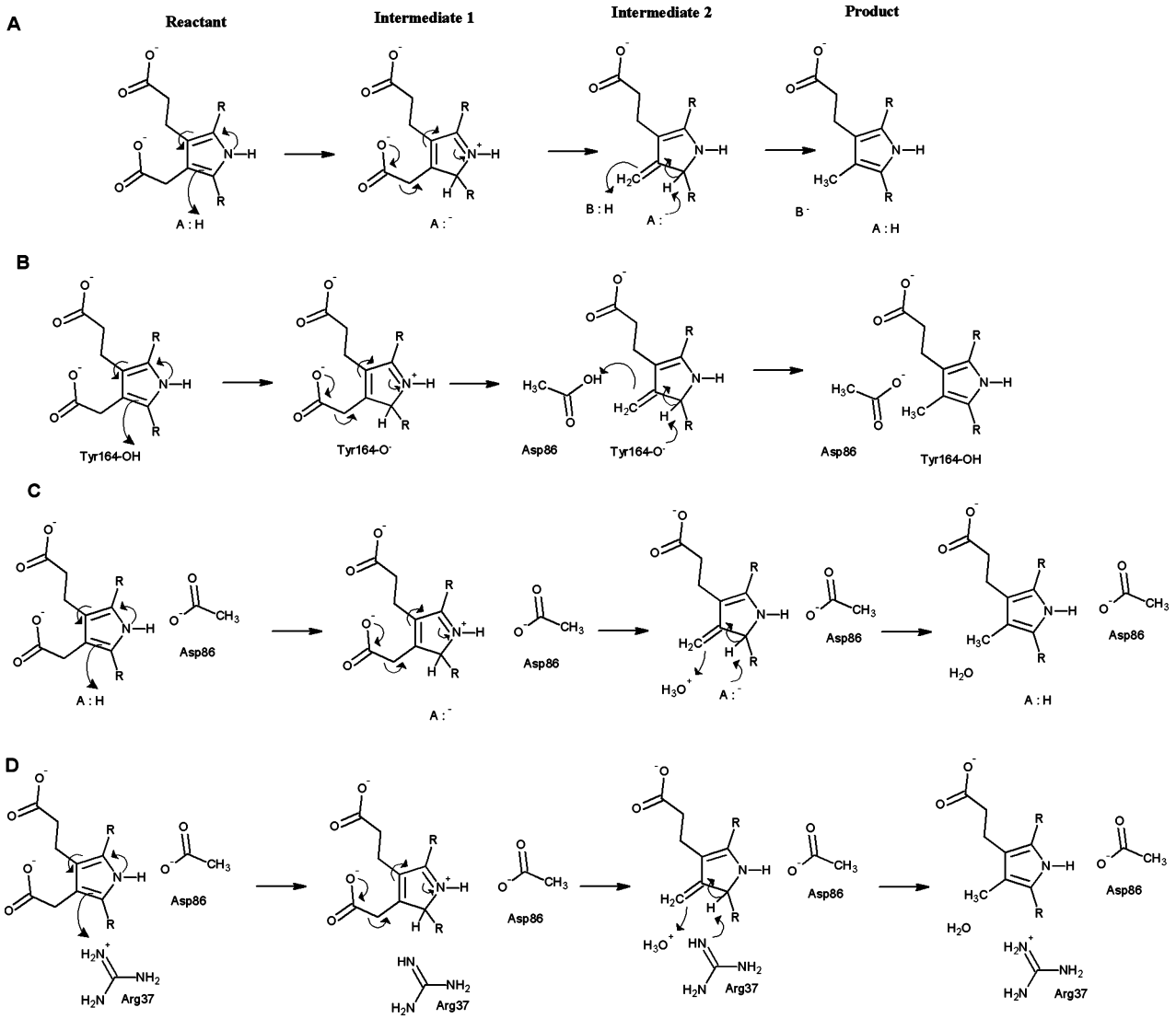

Figure 2. Proposed reaction mechanisms for UroD. (A) Akhtar's model.[7] (B) Martins' model[6] (Tyr164 as first proton donor and Asp86 as second proton donor). (C) Phillips' model[5] (H^+ donation to Asp86-stabilized substrate). (D) Our modification of Phillips' model (Arg37 as H^+ donor to Asp86-stabilized substrate)

carbon atoms. Constraints imposed on the geometries prevented frequency analyses, but for the calculations on our model zero-point and thermal effects ($T = 310.15$ K, $P = 1$ bar) were estimated from calculations on smaller unconstrained models. Contributions for the proton transfer between Arg37 and the substrate were estimated from the proton transfer between guanidinium ion and unsubstituted pyrrole (Figure 3a); an estimate for zero-point and thermal effects for the decarboxylation of the protonated substrate was obtained from the activation $T\Delta S$ of decarboxylation of the related system shown in Figure 3b. A scaling factor of 0.9804 was used for the frequencies.

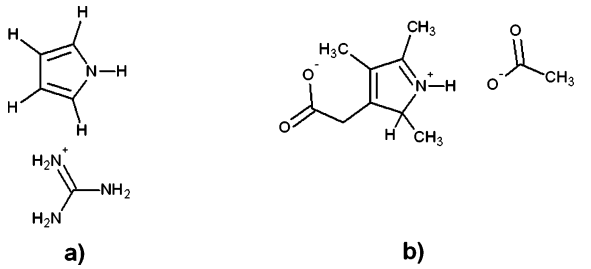

Figure 3. Small models used in the evaluation of zero-point and thermal effects.

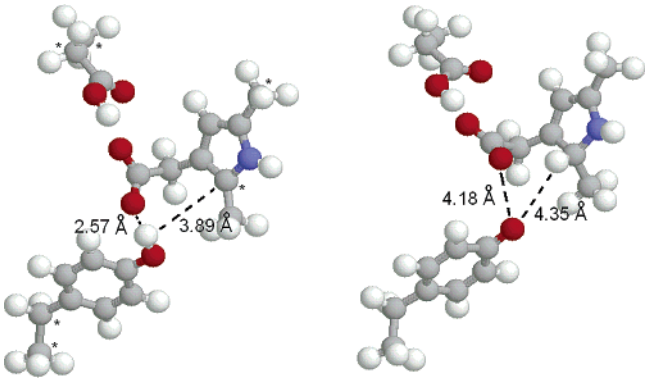

Figure 4. Structures of reactant and product for the proton-transfer step from Tyr164 to the substrate. The labeled atoms were constrained to their crystallographic positions to prevent unrealistic motions.

The polarizable conductor model,[15,16] as implemented in Gaussian03,[17] was used to account for the effects of the protein environment. The dielectric constant was chosen equal to 4, as commonly used for the active site of proteins.[18] Atomic charge and spin density distributions were calculated with a Mulliken population analysis,[19] using the larger basis set. All calculations were performed with the Gaussian03 suite of programs.

III. Results

We started our investigation by analyzing Martins' model, which proved to be unfeasible due to the high energy of several postulated intermediates. We applied several of the insights obtained with this model in order to develop an alternative mechanism, based on Phillips' original proposal.

III.A. Martins' Model (Tyr164 and Asp86 as General Acids). We modeled the side chains of Asp86 as propanoic acid and of Tyr164 as *p*-ethylphenol. In both instances, the Cα and C*β* atoms were kept fixed throughout the calculations to properly account for the restrictions imposed by the polypeptide chain. Our results are shown in Figures 4 and 5, and explained in detail below.

III.A.a. Reactants. On the starting structure, the acetate side chain of the pyrrole ring is stabilized by H-bonds to both Asp86 and Tyr164. This brings the acetate side chain quite close to the phenol hydrogen (1.54 Å), suggesting that its transfer to the pyrrole ring may proceed via this carboxylate. Indeed, we found that the protonated acetate side chain could transfer H^+ to the pyrrole Cα atom without steric strain.

III. A.b. Intermediate 1. Deprotonated Tyr164/Protonated Cα pyrrole atom. Apart from the natural change in hybridization of the pyrrole Cα atom due to its protonation, the most striking changes in the geometry occur in Tyr164. Both Tyr164 and the acetate side chain rotate in order to minimize mutual repulsions due to the negative charge developed on Tyr164, so the distance between the pyrrole carboxylate group and the phenol oxygen atom increases from 2.57 to 4.18 Å. This increased separation of charges would also be allowed in the enzyme, due to the size of the active site cavity. This intermediate lies 35.7 kcal·mol^{-1} above the ground state of the reactant, and its formation would be the rate-limiting step in the mechanism. Separate calculations on Tyr164 alone and the rest of the system show that the small separation between the negative charges observed in this structure is responsible for an electrostatic destabilization of 5.0 kcal·mol^{-1}.

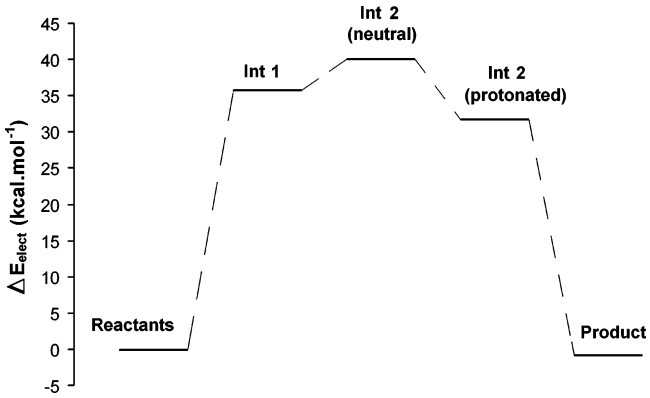

Figure 5. Overall reaction energy profile of uroporphyrinogen III decarboxylation according to Martins' model.

TABLE 1: Relative Electronic Energies (kcal·mol^{-1}) of the Intermediates in the Tyr164-based Model, Calculated at the B3LYP/6-311+G(d,p)//B3LYP/6-31G(d) Level

	gas phase	including solvent effects
reactants	0	0
intermediate 1	50.9	35.7
intermediate 2	44.2	40.0
protonated intermediate 2	66.3	31.7
product	10.3	−0.9

III.A.c. Intermediate 2. Decarboxylated Pyrrole. The decarboxylation of the protonated pyrrole intermediate was found to be slightly endergonic by 4.3 kcal·mol^{-1}. However, the gain in entropy arising from the formation of the gas product will likely offset the decrease of solvent stabilization caused by the formation of two neutral species from a charged molecule (Figure 2B).

III.A.d. Protonation of the Methylene Group by Asp86 and Formation of Neutral Product. Our calculations showed that in the gas phase the neutral form of the substrate present in intermediate 2 is a much weaker base than carboxylate: the calculated structure of deprotonated Asp86/positively charged pyrrole is 22.1 kcal·mol^{-1} higher in energy than the protonated Asp86/neutral pyrrole form. However, in solution the situation is dramatically different: the less delocalized charge in the Asp side chain is much more effectively solvated than the pyrrole ring, so their relative energies change drastically (Table 1). In solution, proton transfer from Asp 86 to the substrate becomes exergonic by 8.3 kcal·mol^{-1}. The return of the proton from the pyrrole ring to Tyr164 yields the neutral, decarboxylated, product. This last step is exergonic by 32.6 kcal·mol^{-1}.

III.B. Our Model (Asp86 as Stabilizing Residue and Arg37 as Proton Donor). At first sight, no amino acid side chains seem to be able to protonate the substrate in the conformation shown in the resolved product-bound crystal structure. Phillips et al.[5] have tentatively suggested that this role might be played by water molecules present in the active site. However, water is a weaker acid than tyrosine, and from the results above it

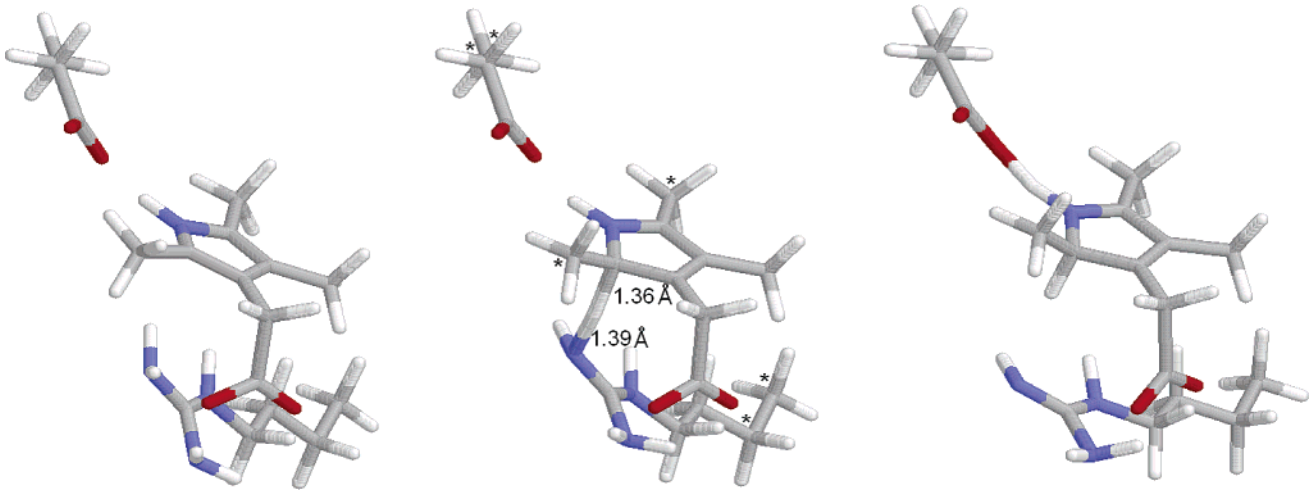

Figure 6. Structures of reactant, transition state, and product for the proton-transfer step from Arg37 to the substrate. The labeled atoms were constrained to their crystallographic positions to prevent unrealistic motions.

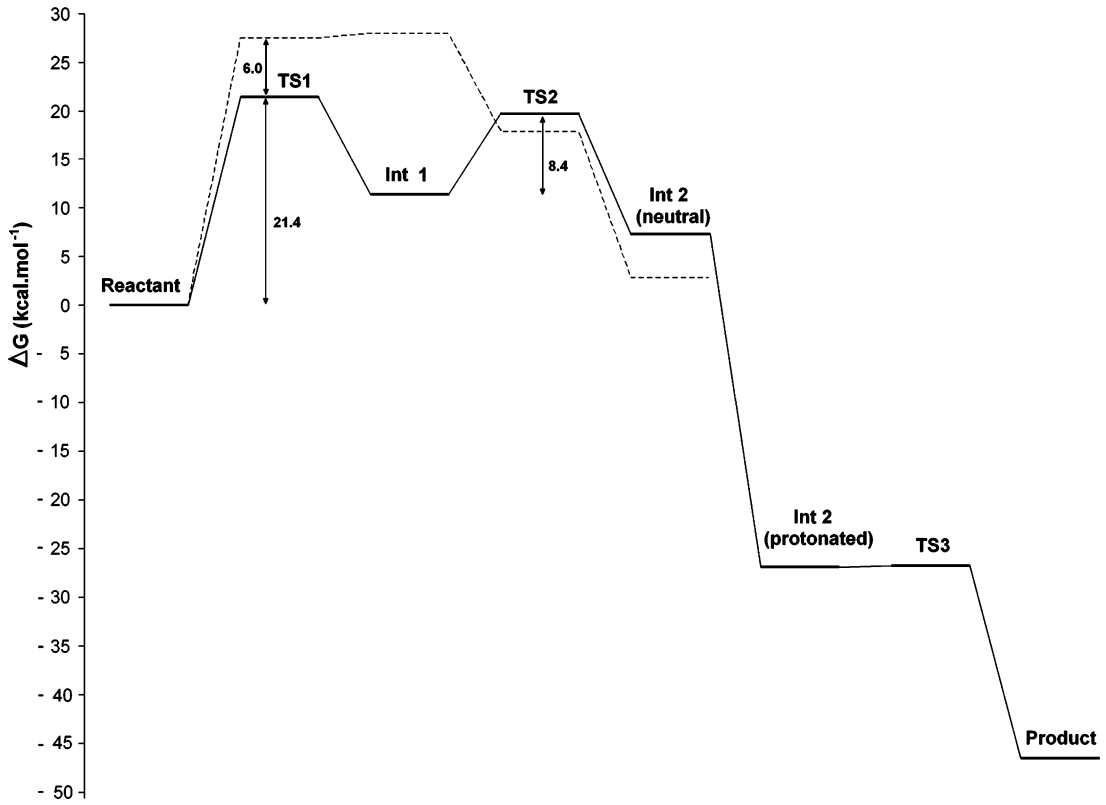

Figure 7. Overall reaction energy profile of uroporphyrinogen III decarboxylation according to our variant of Phillips' model with (—) or without (---) considering the stabilizing effects of Asp86.

can be expected that protonation of the pyrrole by water will be at least more endergonic than 30 kcal·mol^{-1} (=35.7 − 5.0, the energy difference between reactants and intermediate 1 in Martins' model, minus the electrostatic destabilization due to the proximity of the two negative charges), i.e., very slow. A closer inspection of the active site cavity revealed a very flexible arginine residue (Arg37) that might be able to move into close vicinity of the pyrrole rings and to act as a general acid. To test this hypothesis, we performed calculations with models including Asp86 and Arg37. As before, the Cα and Cβ atoms of the side chains, as well as two atoms in the pyrrole substrate, were constrained to their crystallographic positions.

III.B.a. First Step: Proton Transfer from Arg37 to the Pyrrole Ring. In the initial state, the reactive proton in Arg37 lies approximately 2.5 Å from the pyrrole C2 atom. The inherent flexibility of arginine residues allows the proton to approach the pyrrole substrate with relative ease (Figure 6). A very small movement (less than 0.4 Å) of the guanidinium nitrogen atom in Arg37 is enough to bring the proton into the transition state. In this state, the proton lies at almost equal distances from Arg37 (1.39 Å) and the substrate (1.36 Å). As the proton transfer proceeds to completion, the guanidinium group in Arg37 pulls back, eventually settling at an equilibrium position 0.5 Å further from the pyrrole than initially.The electronic barrier for this proton transfer was found to aount to 23.4 kcal·mol^{-1}. Since the constraints imposed on the structure prevented direct determination of zero-point and thermal effects, we estimated them by considering the unconstrained proton transfer from a

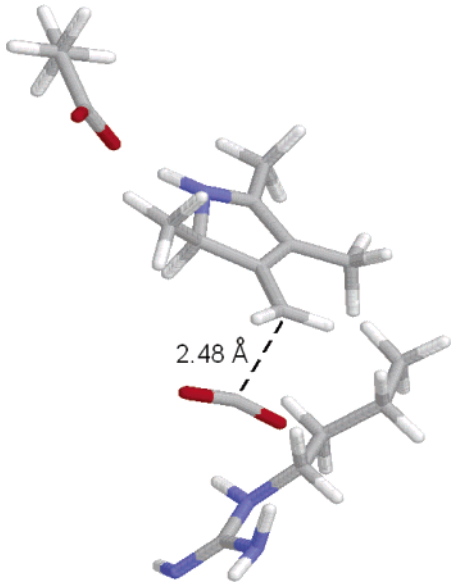

Figure 8. Structure of the transition state of the decarboxylation step.

guanidinium cation to an unsubstituted pyrrole. Addition of these effects (Table 2) to the aforementioned electronic barrier yields an activation ΔG of 21.4 kcal·mol^{-1}, in very good agreement with the experimental value of 19.5 kcal·mol^{-1} (calculated from the values in ref 20). Separate calculations on Asp86 alone and on the rest of the model system show that the assistance of Asp86 is crucial to the enzymatic rate enhancement, since it provides a 6.0 kcal·mol^{-1} stabilization of the charged transition state.

III.B.b. Second Step: Pyrrole Decarboxylation (Figure 8). Surprisingly, we found that, by strongly stabilizing (16.6 kcal·mol^{-1}) the protonated pyrrole, Asp86 actually *hinders* the release of CO_2 from the intermediate: were it not for this stabilization, pyrrole decarboxylation would occur readily without an observable barrier (See Figure 7, dashed line), rather than the calculated electronic barrier of 10.5 kcal·mol^{-1}. After correcting for zero point vibrational energy (ZPVE) and thermal effects (by considering the decarboxylation of a similar, but unconstrained, protonated pyrrole stabilized by a carboxylate−Figure 3b), we found a small activation ΔG of 8.4 kcal·mol^{-1} for this step. The product of this step has formally no charge.

III.B.c. Third Step: Protonation of the Methylene Group in the Decarboxylated Pyrrole. We estimated the Gibbs free energy of the protonation reaction in aqueous solution according to the procedure described by Barone et al.,[21] by adding

TABLE 2: Relative Electronic Energies (kcal·mol^{-1}) of the Described Intermediates in the Arg37-Based Model, Calculated at the B3LYP/6-311+G(d,p)//B3LYP/6-31G(d) Level

	gas phase	solvent effects	ZPVE/thermal effects	total
reactants	0.0			0.0
TS 1	24.2	−0.8	−2.0	21.4
Int 1	14.0	−1.3	−1.3	11.3
TS 2	22.1	1.2	−3.5	19.7
Int 2 (neutral) + CO_2	21.7	−1.1	−13.4	7.3
Int2 (protonated)	−45.0	25.1	−6.5	−26.4
TS 3	−39.4	19.6	−6.5	−26.4
product	−55.7	14.1	−4.6	−46.2

the solvent contribution to the gas-phase value:

$$\Delta G_{\mathrm{aq,AH}} = \Delta G_{\mathrm{gas,AH}} + \Delta\Delta G_{\mathrm{solv,AH}}$$

$$\Delta G_{\mathrm{gas,AH}} = G_{\mathrm{gas,A^-}} + G_{\mathrm{gas,\,H^+}} - G_{\mathrm{gas,AH}}$$

$$\Delta\Delta G_{\mathrm{solv,AH}} = \Delta G_{\mathrm{solv,A^-}} + \Delta G_{\mathrm{solv,\,H^+}} - \Delta G_{\mathrm{solv,AH}}$$

The proton free energy in the gas phase at 310 K and 1 atm is[22]

$$G_{\mathrm{gas,\,H^+}} = 2.5RT - T\Delta S^\circ = 1.54 - 8.13 = -6.59 \text{ kcal·mol}^{-1}$$

For the corresponding value in aqueous solution, $G_{\mathrm{solv,H^+}}$, we used the most recent experimental value (−263.98 kcal·mol^{-1}).[23] According to this scheme, we found the protonation of the methylene group in the decarboxylated pyrrole to be exergonic by more than 33 kcal·mol^{-1}. We did not find any barrier for this proton step in simulations of proton transfer from a hydronium ion to the decarboxylated pyrrole.

III.B.d. Proton Transfer from the Product to Arg37. To prevent artifactual movement of the pyrrole NH proton to Asp86, the N−H distance was kept fixed in the calculations pertaining to this step. Surprisingly, the energetic profile of the H^+ transfer from the product to Arg37 was found to be quite different from the analogous proton transfer from Arg37 to the pyrrole ring. This is probably due to increased inductive effect at C3 due to the conversion of carboxymethyl to a methyl substituent. Proton transfer is mostly barrierless, and exergonic by 19.8 kcal·mol^{-1}. The transition state (Figure 9) is very similar to the one found in the first step, with the proton roughly halfway between Arg37 (1.35 Å) and the product (1.37 Å). The

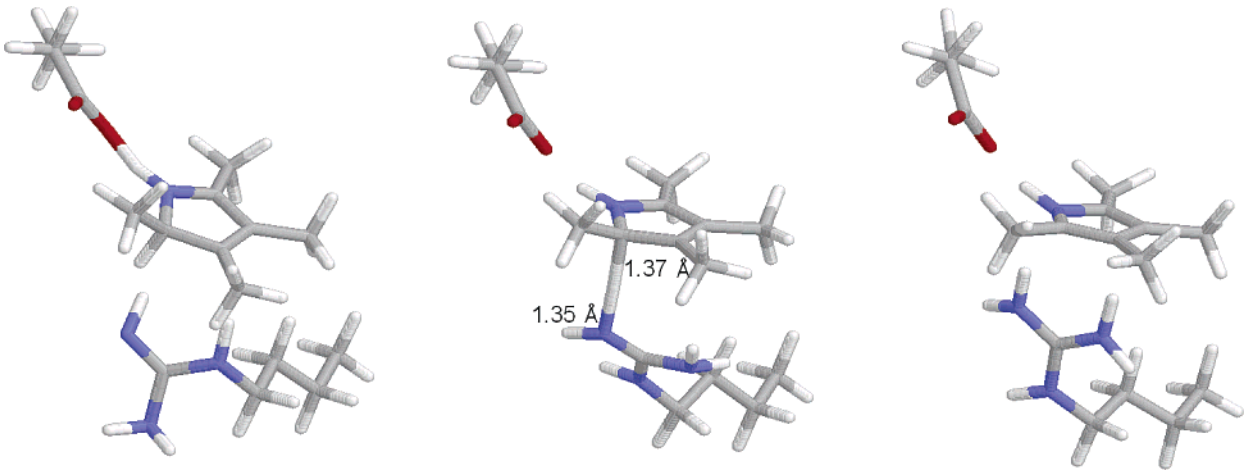

Figure 9. Structures of reactant, transition state, and product for the proton-transfer step from the product to Arg37.

full mechanism is very favorable thermodynamically, with a ΔG of -46.2 kcal·mol^{-1}.

Conclusions

Contrary to expectation in all instances studied (which included charge-stabilized protonated pyrroles, H-bonds stabilizing the leaving carboxylate, gas phase and continuum calculations), we found that pyrrole protonation rather than decarboxylation was the rate-limiting step of this mechanism. This raises the possibility that the enzyme contains a dedicated pyrrole protonation site rather than the specialized "decarboxylation" site optimized to assist CO_2 evolution usually assumed.

Our results show that pyrrole protonation by Tyr164, as proposed in Martins' model, is kinetically unfeasible. In contrast, stabilization of the protonated pyrrole by Asp86 (as proposed in Phillips' model) was found to allow the nearby Arg37 residue to act as a general acid. The activation free energies obtained from this hypothesis are fully consistent with the experimentally observed rate constant, as well as with the known effects of Arg-modifying reagents on the reaction rate.[4] The intervention of an Arg residue as a general acid seems counterintuitive, but Arg residues have been implicated in several enzyme-catalyzed H^+-transfer reactions (inosine 5′-monophosphate dehydrogenase, pectate/pectin lyases, fumarate reductase, L-Asp oxidase, and tyrosine−phenol lyases), as reviewed recently by Guillén Schlippe and Hedstrom.[24] Rather than its ability to function as an acid, in several of these enzymes the problem seems to be instead its ability to function as a base in the initial step, because this implies that it must be present in the neutral form at pH 7, i.e., to have a very low pK_a. Such problems will not occur in our mechanism, since Arg37 starts in its protonated form, which is the dominant form of Arg residues in all but the most pathological instances. Moreover, since the reactive Arg37 is located within a very short distance from all four pyrrole rings present on the substrate, it is possible that this flexible residue successively protonates each of the pyrrole rings, obviating the need for successive 90° rotations of the substrate across its *z*-axis to position the reacting pyrrole in the active site.

Supporting Information Available: Geometries and energies of the reactants, transition states, and products of all chemical reactions. This material is available free of charge via the Internet at http://pubs.acs.org.

References and Notes

(1) Sassa, S.; Kappas, A. *J. Intern. Med.* **2000**, *247*, 169−178.

(2) Wyckof, E. E.; Kushner, J. P. Heme biosynthesis, the porphyrins and the liver. In *The Liver: Biology and Pathobiology*; Arias, I. M., Boyer, J. L., Fausto, N., Jakoby, W. B., Schachter, D. A., Shafritz, D. A. Eds.; Raven Press: New York, 1994; pp 505−527.

(3) Jackson, A. H.; Sancovich, H. A.; Ferramola, A. M.; Evans, N.; Games, D. E.; Matlin, S. A.; Elder, G. H.; Smith, S. G. *Philos. Trans. R. Soc. London, B: Biol. Sci.* **1976**, *273*, 191−206.

(4) Jones, R. M.; Jordan, P. M. *Biochem. J.* **1993**, *293*, 703−712.

(5) Phillips, J. D.; Whitby, F. G.; Kushner, J. P.; Hill, C. P. *EMBO J.* **2003**, *22*, 6225−6233.

(6) Martins, B. M.; Grimm, B.; Mock, H.-P.; Huber, R.; Messerschmidt, A. *J. Biol. Chem.* **2001**, *276*, 44108−44116.

(7) Akhtar, M. *Ciba Found. Symp.* **1994**, *180*, 131−152.

(8) Becke, A. D. *J. Chem. Phys. I* **1993**, *98*, 5648.

(9) Lee, C.; Yang, W.; Parr, R. J. *Phys. Rev. B* **1998**, *37*, 785.

(10) Hertwig, R. W.; Koch, W. *J. Comput. Chem.* **1995**, *16*, 576.

(11) Siegbahn, P. E. M.; Eriksson, L.; Himo, F.; Pavlov, M. *J. Phys. Chem. B* **1998**, *102*, 10622.

(12) Fernandes, P. A.; Ramos, M. J. *J. Am. Chem. Soc.* **2003**, *125*, 6311.

(13) Fernandes, P. A.; Eriksson, L.; Ramos, M. J. *Theor. Chem. Acc.* **2002**, *108*, 352.

(14) Forrester, J.; Frisch, Æ. In *Exploring Chemistry with Electronic Structure Methods*; Gaussian, Inc.; Pittsburgh, PA, 1996; pp 64 and 157.

(15) Barone, V.; Cossi, M. *J. Phys. Chem. A* **1998**, *102*, 1995−2001.

(16) Cossi, M.; Rega, N.; Scalmani, G.; Barone, V. *J. Comput. Chem.* **2003**, 24, 669.

(17) Frisch, M. J.; Trucks, G. W.; Schlegel, H. B.; Scuseria, G. E.; Robb, M. A.; Cheeseman, J. R.; Montgomery, J. A., Jr.; Vreven, T.; Kudin, K. N.; Burant, J. C.; Millam, J. M.; Iyengar, S. S.; Tomasi, J.; Barone, V.; Mennucci, B.; Cossi, M.; Scalmani, G.; Rega, N.; Petersson, G. A.; Nakatsuji, H.; Hada, M.; Ehara, M.; Toyota, K.; Fukuda, R.; Hasegawa, J.; Ishida, M.; Nakajima, T.; Honda, Y.; Kitao, O.; Nakai, H.; Klene, M.; Li, X.; Knox, J. E.; Hratchian, H. P.; Cross, J. B.; Adamo, C.; Jaramillo, J.; Gomperts, R.; Stratmann, R. E.; Yazyev, O.; Austin, A. J.; Cammi, R.; Pomelli, C.; Ochterski, J. W.; Ayala, P. Y.; Morokuma, K.; Voth, G. A.; Salvador, P.; Dannenberg, J. J.; Zakrzewski, V. G.; Dapprich, S.; Daniels, A. D.; Strain, M. C.; Farkas, O.; Malick, D. K.; Rabuck, A. D.; Raghavachari, K.; Foresman, J. B.; Ortiz, J. V.; Cui, Q.; Baboul, A. G.; Clifford, S.; Cioslowski, J.; Stefanov, B. B.; Liu, G.; Liashenko, A.; Piskorz, P.; Komaromi, I.; Martin, R. L.; Fox, D. J.; Keith, T.; Al-Laham, M. A.; Peng, C. Y.; Nanayakkara, A.; Challacombe, M.; Gill, P. M. W.; Johnson, B.; Chen, W.; Wong, M. W.; Gonzalez, C.; Pople, J. A. *Gaussian03*, Revision B.04; Gaussian, Inc.: Pittsburgh, PA, 2003.

(18) Blomberg, M. R. A.; Siegbahn, P. E. M.; Babcock, G. T. *J. Am. Chem. Soc.* **1998**, *120*, 8812.

(19) Mulliken, R. S. *J. Chem. Phys.* **1955**, *23*, 1833.

(20) de Verneuil, H,. Sassa, S.; Kappas, A. *J. Biol. Chem.* **1983**, *258*, 2454−2460.

(21) Barone, V.; Improta, R.; Rega, N. *Theor. Chem. Acc.* **2004**, *111*, 237−245.

(22) McQuarrie, D. A. *Statistical Mechanics*; Harper & Row: New York, 1976.

(23) Tissandier, M. D.; Cowen, K. A.; Feng, W. Y.; Gundluach, E.; Cohen, M. H.; Earhart, A. D.; Coe, J. V.; Tuttle, T. R. *J Phys Chem A* **1998**, *102*, 7787.

(24) Guillén Schlippe, Y. V.; Hedstrom, L. *Arch. Biochem. Biophys.* **2005**, *433*, 266−278.